

Anomalous Paramagnetic Effects in the Mixed State of LuNi₂B₂C

Tuson Park¹, Y. Sun², M. B. Salamon³, A. T. Malinowski¹, M. F. Hundley¹, Eun Mi Choi⁴,
Heon Jung Kim⁴, Sung-Ik Lee⁴, P. C. Canfield⁵, V. G. Kogan⁵, and J. D. Thompson¹

¹*Los Alamos National Laboratory, Los Alamos, New Mexico 87545*

²*Department of Physics and Astronomy, Rice University, Houston, Texas 77005*

³*Department of Physics and Materials Research Laboratory,*

University of Illinois at Urbana-Champaign, Urbana, Illinois 61801

⁴*National Creative Research Initiative Center for Superconductivity and Department of Physics,
Pohang University of Science and Technology, Pohang 790-784, Republic of Korea*

⁵*Ames Laboratory, Department of Physics and Astronomy, Iowa State University, Ames, Iowa 50011*

(Dated: May 12th, 2004)

Anomalous paramagnetic effects in *dc* magnetization were observed in the mixed state of LuNi₂B₂C, unlike any reported previously. It appears as a kink-like feature for $H \geq 30$ kOe and becomes more prominent with increasing field. A specific heat jump at the corresponding temperature suggests that the anomaly is due to a true bulk transition. A magnetic flux transition from a square to an hexagonal lattice is consistent with the anomaly.

In cuprate (high- T_c) superconductors, high-transition temperatures (T_c) and short coherence lengths (ξ) lead to large thermal fluctuation effects, opening a possibility of the melting of the flux line lattice (FLL) at temperatures well below the superconducting transition temperature. A discontinuous step in *dc* magnetization and a sudden, kink-like drop in resistivity signified the first order nature of the melting transition from the vortex lattice into a liquid [1, 2]. In conventional type II superconductors, with modest transition temperatures and large coherence lengths, vortex melting is also expected to occur in a very limited part of the phase diagram [3], but it has yet to be observed experimentally. In the rare-earth nickel borocarbides RNi₂B₂C (R = Y, Dy, Ho, Er, Tm, Lu), the coherence lengths ($\xi \cong 10^2 \text{ \AA}$) and superconducting transition temperatures (16.1 K for R = Lu) lie between these extremes, suggesting that the vortex melting will be observable and may provide further information on vortex dynamics. Indeed, Mun et al. [4] reported the observation of vortex melting in YNi₂B₂C, based on a sharp, kink-like drop in electrical resistivity.

Recently, a magnetic field-driven FLL transition has been observed in the tetragonal borocarbides [5, 6, 7, 8]. The transition from square to hexagonal vortex lattice occurs due to the competition between sources of anisotropy and vortex-vortex interactions. The repulsive nature of the vortex interaction favors the hexagonal Abrikosov lattice, whose vortex spacing is larger than that of a square lattice. The competing anisotropy, which favors a square lattice, can be due to lattice effects (four-fold Fermi surface anisotropy) [9], unconventional superconducting order parameter [10], or the interplay of the two [11, 12]. In combination with non-negligible fluctuation effects, the competition leads to unique vortex dynamics right below the H_{c2} line in the borocarbides, namely a reentrant vortex lattice transition [8]. Fluctuation effects near the upper critical field line wash out the anisotropy effect, stabilizing the Abrikosov hexago-

nal lattice [13, 14]. In this Letter, we report the first observation of paramagnetic effects in the *dc* magnetization M of the mixed state of LuNi₂B₂C. The kink-like feature in M and the corresponding specific heat jump for $H \geq 30$ kOe signify the reentrant FLL transition, which is consistent with the low-field FLL transition line inferred from small angle neutron scattering (SANS) [8].

Single crystals of LuNi₂B₂C were grown in a Ni₂B flux as described elsewhere [15] and were post-growth annealed at $T = 1000$ C° for 100 hours under high vacuum, typically low 10^{-6} Torr [16]. Samples subjected to a preparation process such as grinding, were annealed again at the same condition as the post-growth annealing. A Quantum Design magnetic property measurement system (MPMS) was used to measure *ac* and *dc* magnetization while the heat capacity option of a Quantum Design physical property measurement system (PPMS) was used for specific heat measurements. Electrical resistivity was measured by using a Linear Research *ac* resistance bridge (LR-700) in combination with a PPMS.

The detailed *dc* magnetization of LuNi₂B₂C reveals an anomalous paramagnetic effect for $H \geq 30$ kOe, where the magnetic response deviates from a monotonic decrease and starts to rise, showing decreased diamagnetic response. The in-phase and out-of-phase components of the *ac* susceptibility χ_{ac} show a dip and the specific heat data show a jump at the corresponding temperature, reminiscent of vortex melting in high- T_c cuprates [17]. Electrical transport measurements, however, do not exhibit any feature corresponding to the paramagnetic effect; *e.g.*, a sharp drop in the electrical resistivity. The zero-resistance transition, rather, occurs at a much higher temperature, suggesting that the paramagnetic effect is not related to vortex melting. It is instead consistent with a topological FLL change between square and hexagonal structures.

The top panel of Fig. 1 shows *dc* magnetization M as a function of temperature at several fields. For $H \geq$

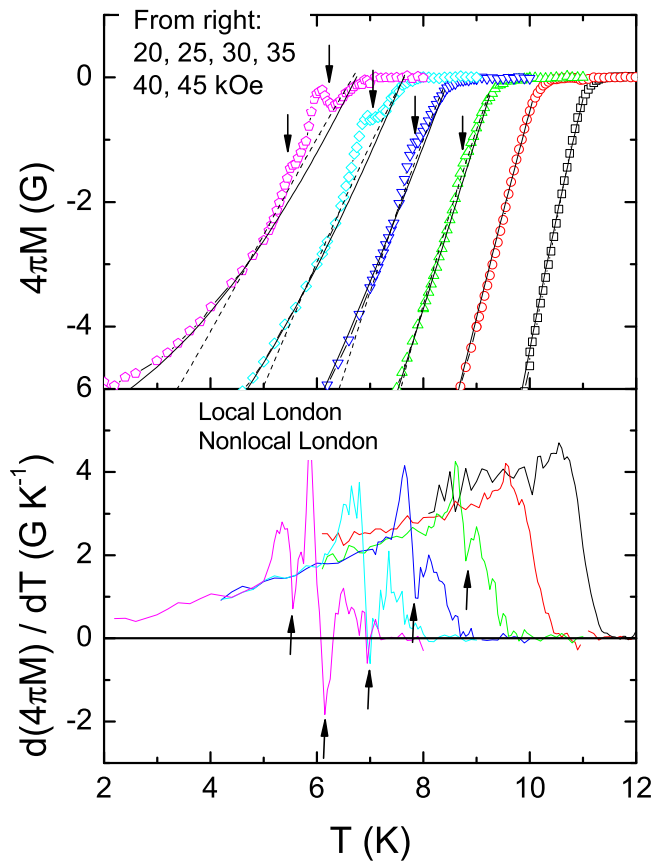


FIG. 1: Top panel: dc magnetization $M(T)$ as a function of temperature at 20, 25, 30, 35, 40, and 45 kOe. Dashed lines are fits from the standard local London model [18] and solid lines from the non-local London model [13] (see text). Bottom panel: temperature derivation of $M(T)$ at corresponding magnetic fields. Arrows indicate the points where kink-like features start to appear

30 kOe, kink-like features appear, which are marked by arrows. The anomalous increase can be easily seen as a sharp drop in dM/dT (arrows in the bottom panel). The magnetization reported here is independent of time and has no hysteresis between zero-field cool (ZFC) and field cool (FC) data within experimental accuracy, indicating that the measured value is an equilibrium magnetization. In the top panel of Fig. 1, we compare the data and some model calculations. Dashed lines are predictions from the standard local London model [18]:

$$-4\pi M = M_0 \ln(\eta H_{c2}/H), \quad (1)$$

where $M_0 = \phi_0/8\pi\lambda^2$, η is a constant of order unity, λ the penetration depth, and ϕ_0 the flux quantum. In the fit, H_{c2} was determined from our resistivity data (see Fig. 2) and M_0 from H_{c2} with $\kappa = \lambda/\xi = 15$. In order to get the best result, the fitting parameter η was varied between 0.95 and 0.97 and the absolute amplitude of M_0 was changed as a function of magnetic field. The local London model explains the monotonic decrease with de-

creasing temperature, but the fit becomes worse at higher field. In a clean system like $\text{LuNi}_2\text{B}_2\text{C}$ where the electronic mean free path is long compared to the coherence length ξ_0 , the current at a point depends on magnetic fields within a characteristic length ρ , or nonlocal radius. Taking into account the nonlocal current-field relation in superconductors, a non-local London model was suggested [19]:

$$-4\pi M = M_0[\ln(1 + H_0/H) - H_0/(H_0 + H) + \Lambda], \quad (2)$$

where $H_0 = \phi_0/(4\pi^2\rho^2)$ and $\Lambda = \eta_1 - \ln(1 + H_0/\eta_2 H_{c2})$ with η_1 and η_2 being order of unity. It is worth noting that the scaling parameter H_{c2} in the local theory is replaced by H_0 in the non-local model. The nonlocal radius ρ slowly decreases with increasing temperature and is suppressed strongly by scattering. The solid lines are best results from the model calculation where we used the temperature dependence of H_0 and Λ from literature for $\text{YNi}_2\text{B}_2\text{C}$ [20]. Both the local and the non-local model explain the temperature dependence of M at low fields while only the non-local model can describe the data at and above 35 kOe. The good fit from the nonlocal model is consistent with the equilibrium magnetization analysis of $\text{YNi}_2\text{B}_2\text{C}$ [20], suggesting the importance of nonlocal effects in the magnetization. The many fitting parameters in both fits, however, prevent us from making a definite conclusion as to which model better describes $M(T)$. Nevertheless, we can extract the important conclusion that the kink-like feature in the mixed state is a new phenomenon that needs further explanation.

In the early stage of high- T_c cuprate research, anomalous paramagnetic effects in $M(T)$ were reported in the irreversible region and this effect was later attributed to the field inhomogeneity of the measured scan length in a SQUID magnetometer [21]. We tested various scan lengths from 1.8 cm to 6 cm for which the field inhomogeneity varies from 0.005 % to 1.4 % along the scan length and found negligible dependence on the measuring length, which suggests that field inhomogeneity is not the source of the anomaly. A more definitive test used a conventional type II superconductor NbSe_2 in a similar configuration. There was no such anomalies in NbSe_2 as in the borocarbide. Taken together, we conclude that the reversible paramagnetic effects are intrinsic to $\text{LuNi}_2\text{B}_2\text{C}$. We also emphasize that the phenomena is different from the paramagnetic Meissner effect (PME) or Wohleben effect [22] where the FC χ becomes positive whereas the ZFC χ remains negative. The PME is an irreversible effect and occurs in the Meissner state, while the subject of this letter is a reversible effect and takes place in the mixed state.

In the top panel of Fig. 2 the reversible magnetization M (left axis) and the out-of-phase component of ac susceptibility χ''_{ac} (right axis) are shown as a function of temperature at 40 kOe. A dip appears both in χ'_{ac} (not shown) and in χ''_{ac} at the same temperature where M

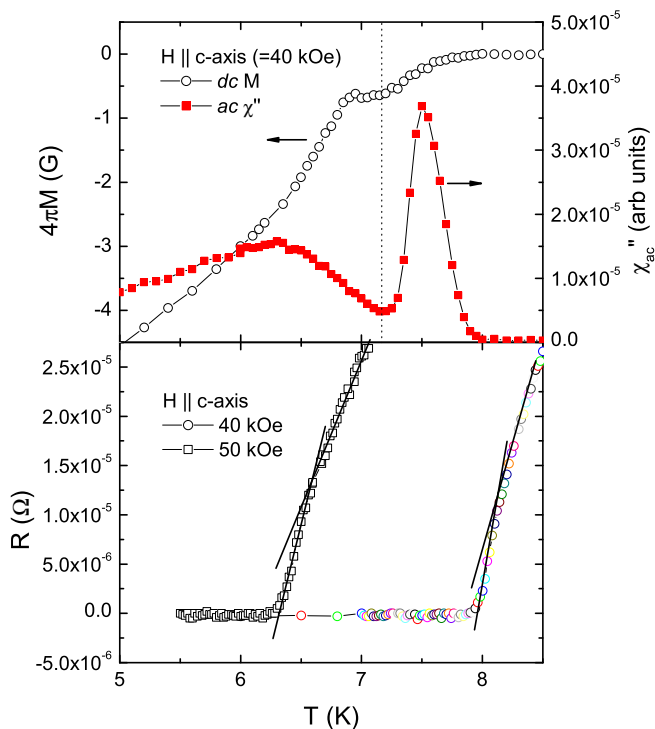


FIG. 2: Top panel: Magnetization (left axis) and the imaginary part of the ac susceptibility (right axis) at 40 kOe. Bottom panel: Resistive superconducting transition at 40 kOe (circles) and 50 kOe (squares). The lines are guide to eyes.

shows the paramagnetic anomaly. Since a dip in χ_{ac} is often related to vortex melting, it is natural to consider the vortex phase change from liquid to lattice or glass as a possible explanation. The resistive superconducting transition at 40 kOe (circles) and 50 kOe (squares) are shown in the bottom panel of Fig. 2. A resistive slope change in the transition region, that can be considered as a signature of the vortex melting [4], was observed at 8.1 K and 6.6 K for 40 kOe and 50 kOe, respectively. The $R = 0$ transition temperature, however, is much higher than the temperature where the dip occurs in χ_{ac} , which argues against the vortex melting scenario as the physical origin of the anomalous paramagnetic effects. The increase in M at the transition temperature is also opposite from the decrease in the vortex melting interpretation. Recently, a structural phase transition in FLL was suggested to explain another peak effect observed below the vortex melting line in YBCO [23, 24]. The vanishing of a *squash* elastic mode gives rise to a topological FLL transition and leads to the new peak effect while the softening of the shear modes c_{66} is relevant to the conventional peak effect in high- T_c cuprates [25]. The observation of the dip effect well below the melting line in $\text{LuNi}_2\text{B}_2\text{C}$ indicates that the anomalous paramagnetic effects is related to a change in the FLL and the increase in M is also consistent with the FLL change where the

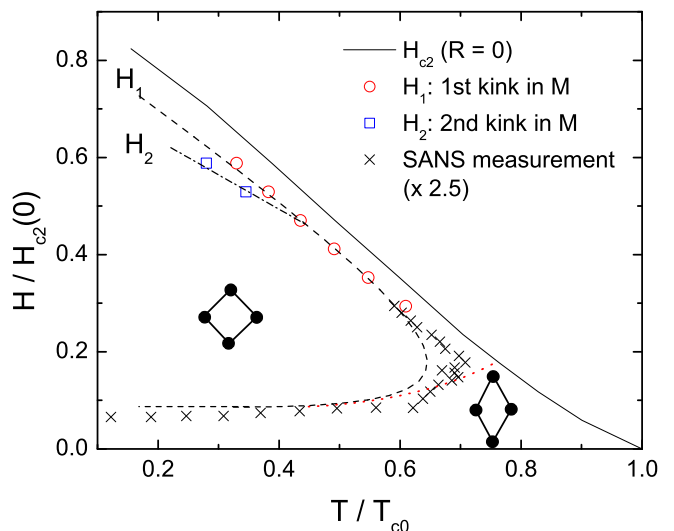


FIG. 3: $H - T$ phase diagram. The upper critical field H_{c2} was determined from the resistive transition (solid line). The H_1 line indicates the temperature where $M(T)$ deviates from a monotonic decrease and the H_2 line is where the second anomaly occurs above 45 kOe. The dashed line depicts qualitatively what the fluctuations models based on the nonlocal London [13] or extended GL [14] predict. The dotted line is from theories without fluctuation effects [27, 28]. The crosses are SANS data [8] where the value was multiplied by 2.5 for comparison. The square and rhombic shapes are forms of vortex lattices.

Abrikosov geometrical factor β_A changes [18, 26].

The $H-T$ phase diagram is shown in Fig. 3. The upper critical field line H_{c2} was determined from the $R = 0$ superconducting transition and is consistent with the temperature where χ_{ac} starts to have a non-zero value. The H_1 line in the mixed state is the point where the reversible magnetization shows the paramagnetic effects and H_2 is the 2nd anomaly that appears above 45 kOe (Fig.1). Recently, small angle neutron scattering (SANS) at low fields found a hexagonal FLL in the region just below the upper critical field line, indicating a reentrant field-driven FLL transition (crosses in Fig. 3) [8]. Fluctuation effects in the vicinity of the H_{c2} line were considered to explain the unexpected behavior. According to the Gurevich-Kogan non-local London model [13], the anisotropic nonlocal potential, which is responsible for the low-field FLL transition, is averaged out by thermal vortex fluctuations near H_{c2} . Since the interaction becomes isotropic, the hexagonal Abrikosov lattice is preferable, leading to the second FLL transition from square back to rhombic (triangular) lattice as the field gets closer to the H_{c2} line. The reentrant transition is predicted to occur well below the vortex melting line because the amplitude of vortex fluctuations required to wash out the nonlocal effects is much smaller than that for the vortex melting. This prediction is consistent with our observation that the H_1 line is much below the $R = 0$ transi-

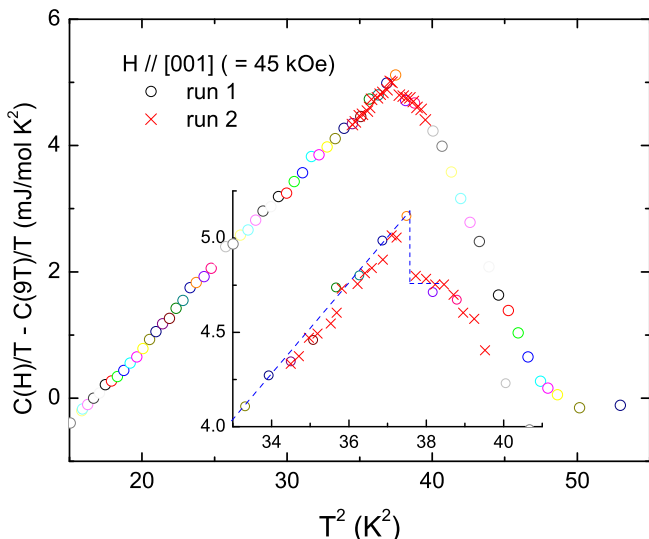


FIG. 4: Specific heat difference $C(H)/T - C(9T)/T$ vs T^2 at 45 kOe for $H \parallel [001]$. Inset: blow-up of the main panel at 6.1 K. The dashed line is a guide to the eye.

tion line. The dashed line depicts qualitatively what the fluctuations models based on the nonlocal London [13] or extended GL [14] predict, which nicely explains the H_1 line. The dotted line is the FLL transition line that crosses the H_{c2} line both in the non-local London model [27] and in the extended Ginzburg-Landau (GL) theory [28] without fluctuation effects.

For vortex melting, where the lattice changes to a liquid, the transition involves latent heat and the specific heat shows a sharp peak at the transition temperature [17]. For a vortex structural transition from square to hexagonal lattice, we expect a similar anomaly in specific heat. Fig. 4 shows the specific heat data of $\text{LuNi}_2\text{B}_2\text{C}$ at 45 kOe as a function of temperature. In addition to the superconducting transition between 6.22 and 6.89 K, another specific heat jump was, indeed, observed at 6.12 K which corresponds to the anomalous paramagnetic effects. The inset, which magnifies the data at the transition temperature, clearly shows the additional jump. The entropy change involved in the transition was estimated to be 0.04 mJ/mol·K, where we subtracted the linear part of the specific heat below T_c . The additional specific heat anomaly at 40 and 50 kOe were also observed at the temperatures corresponding to the paramagnetic effects in H_1 . We note that we were not able to discern any corresponding feature to the H_2 line in C_p or in χ_{ac} . More work is in progress to understand the 2nd anomalous feature in M for $H \geq 45$ kOe.

In summary, we report the first observation of an anomalous paramagnetic effect in the magnetization of the mixed state in $\text{LuNi}_2\text{B}_2\text{C}$. A dip appears in χ_{ac} at the same temperature as the paramagnetic effects, suggesting the relevance of the flux line lattice. The $H - T$

phase diagram is consistent with a FLL structural transition from square to hexagonal lattice just below the upper critical field line. The observation of the additional specific heat jump at the corresponding temperature underscores the interpretation of paramagnetic effects as due to the reentrant FLL transition in $\text{LuNi}_2\text{B}_2\text{C}$.

The work at Los Alamos was performed under the auspices of the U.S. Department of Energy (DOE) and at Urbana under NSF Grant No. DMR 99-72087. The work at Pohang was supported by the Ministry of Science and Technology of Korea through the Creative Research Initiative Program and at Ames by Iowa State University of Science and Technology under DOE Contract No. W-7405-ENG-82. We acknowledge benefits from discussion with Lev N. Bulaevskii, M. P. Maley, and I. Vekhter. We thank T. Darling for assistance in sample annealing.

-
- [1] E. Zeldov, D. Majer, M. Konczykowski, V. B. Geshkenbein, V. M. Vinokur, and H. Shtrikman, *Nature (London)* **375**, 373 (1995).
 - [2] U. Welp, J. A. Fendrich, W. K. Kwok, G. W. Crabtree, and B. W. Veal, *Phys. Rev. Lett.* **76**, 4809 (1996).
 - [3] G. Eilenberger, *Phys. Rev.* **164**, 628 (1967).
 - [4] M.-O. Mun, S.-I. Lee, W. C. Lee, P. C. Canfield, B. K. Cho, and D. C. Johnston, *Phys. Rev. Lett.* **76**, 2790 (1996).
 - [5] U. Yaron, P. Gammel, D. Huse, R. Kleiman, C. Oglesby, E. Bucher, B. Batlogg, D. Bishop, K. Mortensen, and K. Clausen, *Nature (London)* **382**, 236 (1996).
 - [6] M. R. Eskildsen, K. Harada, P. L. Gammel, A. B. Abrahamsen, N. H. Andersen, G. Ernst, A. P. Ramirez, D. J. Bishop, K. Mortensen, D. G. Naugle, et al., *Nature (London)* **393**, 242 (1998).
 - [7] H. Sakata, M. Oosawa, K. Matsuba, N. Nishida, H. Takeya, and K. Hirata, *Phys. Rev. Lett.* **84**, 1583 (2000).
 - [8] M. R. Eskildsen, A. B. Abrahamsen, V. G. Kogan, P. L. Gammel, K. Mortensen, N. H. Andersen, and P. C. Canfield, *Phys. Rev. Lett.* **86**, 5148 (2001).
 - [9] V. G. Kogan, M. Bullock, B. Harmon, P. Miranovic, L. Dobrosavljevic-Grujic, P. L. Gammel, and D. J. Bishop, *Phys. Rev. B* **55**, R8693 (1997).
 - [10] R. Gilardi, J. Mesot, A. Drew, U. Divakar, S. L. Lee, E. M. Forgan, O. Zaharko, K. Conder, V. K. Aswal, C. D. Dewhurst, et al., *Phys. Rev. Lett.* **88**, 217003 (2002).
 - [11] N. Nakai, P. Miranovic, M. Ichioka, and K. Machida, *Phys. Rev. Lett.* **89**, 237004 (2002).
 - [12] T. Park, E. E. M. Chia, M. B. Salamon, E. D. Bauer, I. Vekhter, J. D. Thompson, E. M. Choi, H. J. Kim, S.-I. Lee, and P. C. Canfield, *Phys. Rev. Lett.* (2004), in press.
 - [13] A. Gurevich and V. G. Kogan, *Phys. Rev. Lett.* **87**, 177009 (2001).
 - [14] A. D. Klironomos and A. T. Dorsey, *Phys. Rev. Lett.* **91**, 097002 (2003).
 - [15] B. K. Cho, P. C. Canfield, L. L. Miller, D. C. Johnston, W. P. Beyermann, and A. Yatskar, *Phys. Rev. B* **52**, 3684 (1995).
 - [16] X. Y. Miao, S. L. Bud'ko, and P. C. Canfield, *J. Alloys*

- Comp. **338**, 13 (2002).
- [17] A. Schilling, R. A. Fisher, N. E. Phillips, U. Welp, W. K. Kwok, and G. W. Crabtree, Phys. Rev. Lett. **78**, 4833 (1997).
- [18] P. G. deGennes, *Superconductivity of Metals and Alloys* (Benjamin, New York, 1966).
- [19] V. G. Kogan, A. Gurevich, J. H. Cho, D. C. Johnston, M. Xu, J. R. Thompson, and A. Martynovich, Phys. Rev. B **54**, 12386 (1996).
- [20] K. J. Song, J. R. Thompson, M. Yethiraj, D. K. Christen, C. V. Tomy, and D. M. Paul, Phys. Rev. B **59**, R6620 (1999).
- [21] A. Schilling, H. R. Ott, and T. Wolf, Phys. Rev. B **46**, 14253 (1992).
- [22] W. Braunisch, N. Knauf, G. Bauer, A. Kock, A. Becker, B. Freitag, A. Grutz, V. Kataev, S. Neuhausen, B. Roden, et al., Phys. Rev. B **48**, 4030 (1993).
- [23] K. Deligiannis, Phys. Rev. Lett. **79**, 2121 (1997).
- [24] B. Rosenstein and A. Knigavko, Phys. Rev. Lett. **83**, 844 (1999).
- [25] A. I. Larkin, M. C. Marchetti, and V. M. Vinokur, Phys. Rev. Lett. **75**, 2992 (1995).
- [26] A. A. Abrikosov, Sov. Phys. JETP **5**, 1174 (1957).
- [27] I. Affleck, M. Franz, and M. H. S. Amin, Phys. Rev. B **55**, R704 (1997).
- [28] Y. DeWilde, M. Iavarone, U. Welp, V. Methushko, A. E. Koshelev, I. Aranson, G. W. Crabtree, and P. C. Canfield, Phys. Rev. Lett. **78**, 4273 (1997).